Trans. Indian Inst. Met.
Vol. 61, No. 4, August 2008, pp. 279-282

TP 2221

Heat Flux Transients At The Solder/Substrate Interface In Dip Soldering

Shankargoud Nyamannavar and K. Narayan Prabhu
Department of Metallurgical & Materials Engineering
National Institute of Technology Karnataka
Surathkal, Srinivasnagar, Mangalore 575 025, India
E-mail: prabhukn_2002@yahoo.co.in
(Received 6 June 2007 ; in revised form 26 February 2008)

ABSTRACT

In the present work an experimental set-up was designed to simulate the dip soldering conditions. The set-up was used to estimate heat flux transients at the solder/substrate interface during solidification of Sn 3.5Ag solder against copper substrate. The inverse heat conduction problem (IHCP) was solved in the substrate region for estimation of heat flux transients. A reasonably good agreement between measurements and model predictions was achieved validating the inverse model. The computer code developed in the present study could be used to assess the effect of process variables on contact heat flux at the solder/substrate interface.

1. INTRODUCTION

Quantification of the heat transfer boundary conditions in the metallurgical process like soldering can be quite challenging, due to rapid non-linear changes in the heat flux with time. During soldering the bonding is achieved by wetting of the solder alloy to the base metal and the process involves neither diffusion nor the melting of base metal[1]. The conditions are similar to the metal solidification in conventional casting. Therefore techniques that are used for estimation of heat flux transients in casting process can be used to asses the heat transfer during soldering process. Several researchers have attempted to measure the interfacial heat flux, utilizing measured temperatures in both casting and mold materials, by inverse heat conduction (IHC) method for metal casting processes[2-10]. In these methods, the boundary heat flux is not known initially but is calculated from the temperature-time history in the mold at a known location during casting solidification.

An attempt has been made in the present work to design an experimental set-up to simulate the dip soldering process. A computer program based on FEM and Beck's method[11] was developed for estimation of non-linear heat flux at the solder/substrate interface. Heat flow analysis was carried out for dip soldering conditions characterized by solidification of a lead free Sn 3.5Ag solder alloy against a copper substrate.

2. EXPERIMENTAL

To simulate the dip soldering process, a cylindrical copper probe of 10 mm diameter and 40 mm height was dipped in the Sn 3.5Ag solder liquid. The probe was instrumented with a K-type mineral insulated thermocouple at the center through 1.5 mm diameter hole. The thermocouple response time was found to be 0.4 s. The thermocouple was connected to a data logger (NI SCXI1000) and the probe temperature was measured for every 0.01 second. About 1 kg of Sn 3.5Ag solder alloy was taken in a clay graphite crucible and melted in an electric resistance furnace. Experiments were carried out under similar conditions to assess the repeatability. A schematic sketch of the experimental set-up is shown in Fig. 1. A temperature drop of about 10 K was observed after the dipping of the copper probe in the liquid melt.

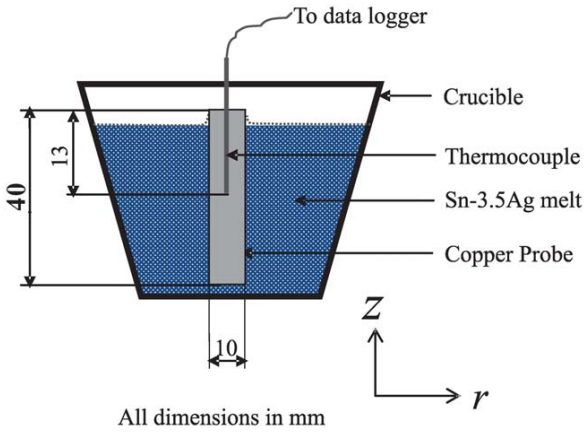

Fig. 1 : Schematic two dimensional sketch of the experimental set-up

3. THEORETICAL BACKGROUND

Inverse heat conduction problem was solved in the substrate region to obtain the heat flux transients at solder substrate interface. The IHC analysis estimates the heat-transfer boundary condition, based on the measured temperature history at known interior location in the substrate material. In the present analysis, the thermal properties specific heat, conductivity and density were assumed to be constant. Temperature measurements were smoothed to stabilize the solution of inverse problem. Computer code was developed using computer programming language 'C' for IHC analysis.

Heat transfer in a three dimensional domain Ω with geometric symmetry about the z axis can be formulated conveniently in a two dimensional coordinate r, z domain. If, in addition, all heat transfer and thermal properties are independent of q,

then the temperature is a function of only r and z, and the three dimensional domain can be represented as two dimensional domain and analyzed for heat conduction. The finite element formulation and derivation of element matrices is similar to the plane triangular element; the principle difference is that integrations are carried out in the r-z plane and in cylindrical coordinates[12]. The two dimensional axi-symmetric heat conduction equation for an isotropic material is given by

$$\frac{1}{r}\frac{\partial}{\partial r}\left(r\frac{\partial T}{\partial r}\right)+\frac{\partial}{\partial z}\left(\frac{\partial T}{\partial z}\right)=\frac{\rho C_p}{k}\frac{\partial T}{\partial t} \quad (1)$$

where k thermal conductivity ρ is density of probe material, C_p is specific heat of probe material and T temperature. Material properties k, ρ and C_p were assumed to be constant. The two dimensional axi-symmetric heat conduction eq. (1) can be solved by FEM subject to the initial condition

$$T = T_0(r,z,0) \text{ in } \Omega \quad (2)$$

and the following boundary (G) conditions.

$$T_s = T_1(r,z,t) \quad (3)$$

$$kr\frac{\partial T}{\partial r}n_r + kr\frac{\partial T}{\partial z}n_z + rq = 0\,, \quad (4)$$

$$kr\frac{\partial T}{\partial r}n_r + kr\frac{\partial T}{\partial z}n_z - rh(T_\Gamma - T_\infty) = 0\,, \quad (5)$$

$$kr\frac{\partial T}{\partial r}n_r + kr\frac{\partial T}{\partial z}n_z - r(\sigma\varepsilon T_\Gamma^4 - \alpha q_R) = 0 \quad (6)$$

where T_0 is the initial temperature of the probe before dipping in the liquid solder, T_1 is the specified surface temperature, n_r and n_z are the direction cosines of the outward normal to the bounding curve Γ, q is the heat flow per unit area (unknown heat flux) at the surface of the probe which is in contact with liquid solder, and $h(T_\Gamma - T_\infty)$ is the heat loss at the top surface of the probe, which is exposed to air, due to convection to the ambient temperature T_∞ with convection heat transfer coefficient h, T_Γ is unknown boundary temperature, σ is the Stefan-Boltzman constant, ε is the surface emissivity, α is the surface absorptivity and Q_R is incident radiant heat flow rate per unit area. In present study the radiation heat transfer was neglected and there is no specified temperature at the boundary. Therefore the boundary conditions eq.(3) and eq.(6) were not considered for formulation of inverse thermal analysis.

The solution domain Ω was divided into regular mesh of M (=1600) right angle isosceles triangle elements of height 0.5 mm and width 0.5 mm (Fig. 2). The temperature variation over each element was approximated by linear interpolation functions and the finite element equation was derived from eq. (1) by Galerkin Method. The numerical solution for transient heat transfer was carried out by implicit numerical integration method with backward difference recursion analysis[12].

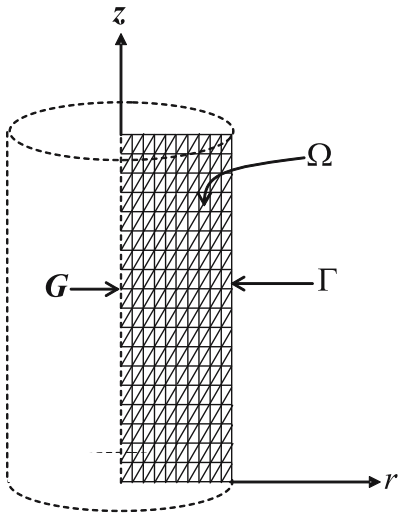

Fig. 2 : Two-dimensional axi-symmetric representation and finite element discretization of cylindrical metal probe for FEM analysis.

The spatial distribution of heat flux q on the probe surface in contact with solder liquid was neglected. The q was estimated at each time step assuming single value of q over entire solder/probe interface. The heat flux q, at any time t on boundary Γ can be estimated by Beck's[11] non-linear estimation technique. The method involves minimization of the function

(7)

The problem is to find the value of the q, which minimizes the sum of the squared deviations of the experimental temperatures from the estimated temperatures. The terms Y_{n+i} and T_{n+i} are measured and calculated temperatures at locations G at time $(n+i)$. T_{n+i} is temperature at G obtained form numerical solution using finite element method. The objective is to calculate the q using temperatures T_{n+1}, T_{n+2}, $\ldots T_{n+m}$ (which are associated with the time interval for q) plus the temperatures T_{n+m+1}, T_{n+m+2},$\ldots\ldots T_{n+m+mp}$. The latter temperatures are called future temperatures, where p is a small integer.

Assuming q^l is known (q^1=1 initially), q^{l+1} was estimated as follows. The function $F(q)$ was minimized by an iterative procedure using Taylors series expansion.

$$T^{l+1} \approx T^l + \frac{\partial T^l}{\partial q^l}\left(q^{l+1} - q^l\right) \quad (8)$$

The subscript l denotes the iteration step. The partial derivative $\partial T^l/\partial q^l$ is the sensitivity coefficient ϕ. It was calculated using

$$\phi^l = \frac{T\left(q^l(1+\varepsilon)\right) - T\left(q^l\right)}{\varepsilon q^l} \quad (9)$$

The temperature T is estimated by finite element method twice with q^l and then with $q^l(1+\varepsilon)$ where ε is a small number and was taken as 0.001.

Introducing eq. (8) in eq. (7) and applying the minimization condition $\partial F/\partial q=0$ gives the correction in q at each iteration step

$$\nabla q^l = \frac{\sum_{i=1}^{mp}\left(Y_{n+i} - T^l_{n+i}\right)\phi^l}{\sum_{i=1}^{mp}\left(\phi^l\right)^2} \tag{10}$$

where $\nabla q^l = q^{l+1} - q^l$

The procedure was repeated for few flux values. The iteration was continued until say

$$\frac{\nabla q^l}{q^l} < 0.005 \tag{11}$$

A small value of 0.005 was used to test convergence in the estimated heat flux value. The estimated value of heat flux for different values of convergence criterion 0.001, 0.0005 and 0.0001 showed similar values. Therefore 0.005 was used as convergence criterion for estimation of heat flux. The calculation of the heat flux as a function of time was continued until the end of the desired period. The heat flux was estimated for every 0.1 second. The detailed flow diagram for estimation of q is shown in Fig. 3.

Numerical analysis was carried out using different element sizes for the same experimental conditions. The heat flux transients were estimated for solution domain divided into 1024, 1600 and 2304 elements. The maximum percentage difference in heat flux estimated at 1600 and 2304 triangles was found to be less than 0.4%. Therefore the division of solution domain into 891 nodes and 1600 elements was sufficient for element size independent solution of the inverse problem.

The density, thermal conductivity and specific heat of copper substrate used in the simulation are 8920 kg/m^3, 398 W/mK and 380 J/kg K respectively[13]. The ambient temperature of air surrounding the probe during dipping was found to be about 313 K. The heat transfer coefficient h for convective heat transfer at the probe surface exposed to the air was estimated assuming natural convection[14]. The value of h varies with temperature of the probe and the probe temperature increases from room temperature (~300 K) to the liquid solder temperature (~508 K). Heat flux transients were estimated using different values of h and the maximum percentage difference between heat flux values estimated with different h values was less than 0.5%. Hence a single value of h (=14.5 W/m^{2}K) corresponding to the mean temperature (~423 K) of the probe was used.

4. RESULTS AND DISCUSSION

The measured and estimated temperatures (Y and T) obtained by solving inverse heat conduction problem in the copper probe are shown in Fig. 4. A good agreement is obtained between measured and estimated temperatures.

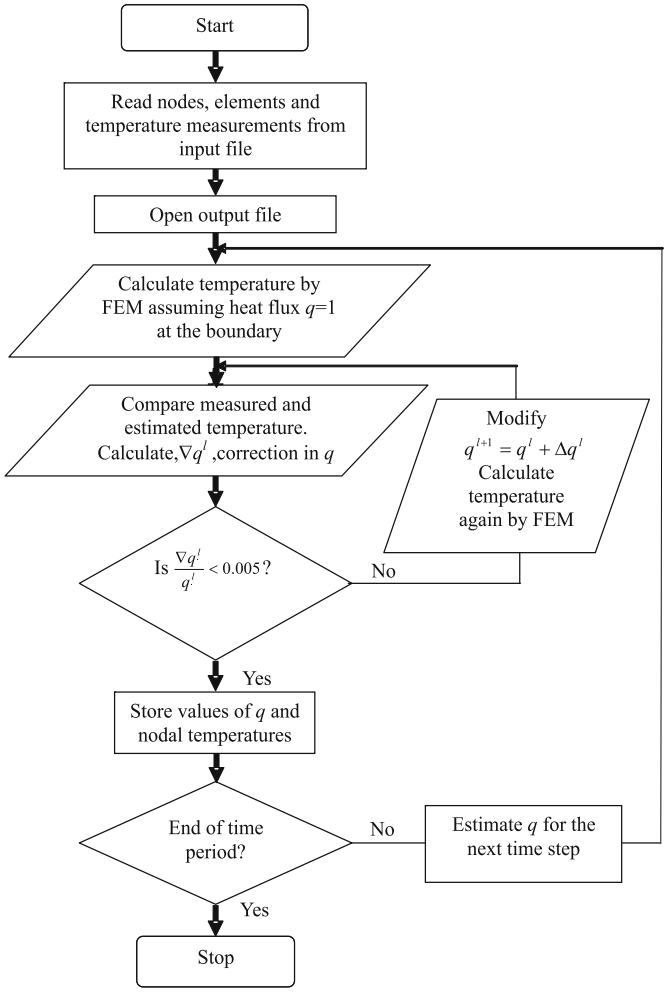

Fig. 3 : Flow diagram for non-linear estimation of heat flux at the boundary

The variation of heat flux at the solder/substrate interface for copper probe dipped in Sn 3.5Ag solder is shown in Fig. 5. The heat flux increases rapidly with time initially and reaches a peak value of 496 kW/m^2 (a). The heat flux then decreases with time and reaches minimum value of 16 kW/m^2 (b) when the probe temperature is about 492 K. The heat flux increases once again and reaches a second peak 30 kW/m^2 (c) and decrease to very low values thereafter.

Initially when the test probe is dipped in the liquid solder, it comes in contact with liquid metal. Since the process of dipping is progressive one, the liquid metal takes some time to fully cover the metal surface and establish proper contact. Therefore the heat flux increases from low value and reaches a peak due to increase in contact area between the liquid solder and metal surface. Meanwhile the liquid that comes in contact with the metal surface gets solidified and forms a solid shell. The formation of solid shell transforms the interface from a solid-liquid to solid–solid contact. This change is associated with decrease in the thermal contact conductance (heat transfer coefficient)[3]. The decrease in heat transfer coefficient and the continuous decrease in the temperature difference (ΔT) between the probe surface and surrounding liquid solder, results in the decrease in the heat

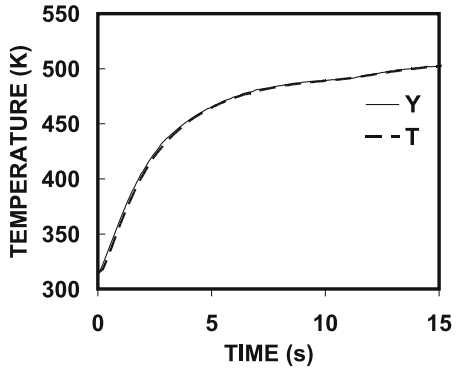

Fig. 4 : Comparison of measured and estimated temperatures

flux with time. Hence during dipping two competing phenomena are active at the interface; (i) the increasing contact area between the melt and the substrate surface (ii) change in the nature of contact at the solder/substrate from a solid-liquid to solid–solid contact with progress in solidification. Initially the increase in contact area is more dominant and therefore the heat flux increases. Once the probe is dipped completely in the liquid, there is no further increase in the contact area and the formation of stable solid shell at the interface becomes a dominant factor affecting heat transfer. Therefore heat flux initially increases, reaches a peak (a) and then decreases with time due to the formation of solid shell at the interface accompanied by a continuous decrease in the temperature difference between the probe and surrounding liquid solder. The solid shell grows in thickness with time and offers more resistance to heat flow which further decreases heat flux.

The decrease in heat flux with time after the initial peak value continues till the substrate temperature reaches the eutectic temperature (494 K) of the solder alloy (b). As the temperature of the substrate approaches eutectic temperature of the solder, the solidified shell starts remelting, changing the nature of interface back from solid-solid to solid-liquid. The remelting of solid shell increases the heat transfer coefficient at the interface and therefore results in the momentary increase in the heat flux and appearance of a second peak (c). The appearance of second peak in the heat flux transients is attributed to the dynamics of solder solidification at the interface. During remelting of solid shell there will be two

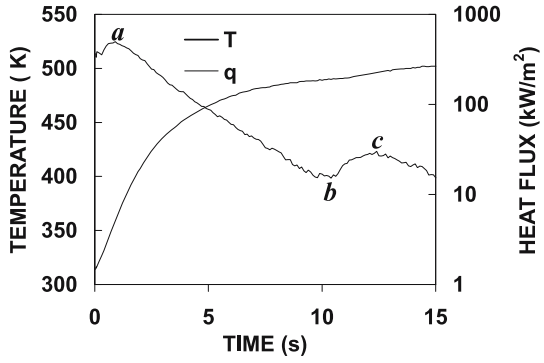

Fig. 5 : Probe surface temperature and heat flux transients at the interface estimated by inverse analysis

competing phenomena active at the interface; (i) the increasing thermal contact conductance between melt and the substrate surface (ii) decreasing temperature difference between the melt and the substrate surface. Once the solid shell melts completely there is no further increase in the thermal contact conductance. The heat flux transients decrease with time to very low values once again after reaching second peak (c) due to decrease in temperature difference between the substrate and liquid solder.

5. CONCLUSIONS

An experimental set up was designed to simulate the dip soldering process. The phenomenon of evolution of heat flux transients at the solder/substrate interface was analyzed by carrying out experiments with copper probe and Sn 3.5 Ag solder alloy. Heat flux increases rapidly with time initially reaches peak (496 kW/m^2) and decreases with time and reaches a minimum (16 kW/m^2). The heat flux increases again, once the probe temperature reaches a value corresponding to the eutectic temperature of the solder alloy, and attains a second peak (30 kW/m^2). The appearance of minimum and second peak in the heat flux transients is attributed to the dynamics of solder solidification at the interface.

The experimental set-up designed and the computer program developed in the present study could be used to estimate heat flux transients at the solder/substrate interface. The effect of process variables like substrate and solder material, soldering flux, probe diameter and other factors on contact heat flux at the solder/substrate interface is yet to be investigated.

ACKNOWLEDGEMENTS

The authors thank Defense Research Development Organization (DRDO), Government of India, New Delhi for the financial assistance under a R & D project grant (No. ERIP/ER/0304272/M/01).

REFERENCES

1. Manko H H, Solders and Soldering, 3rd Ed. McGraw Hill Inc, New York (1992).
2. Muojekwu C A, Samarasekara I V, Brimacombe J K, *Met Mat Trans*, **26B** (1995) 361.
3. Wang W, Qiu H H, *Int J Heat and Mass Trans*, **45** (2002) 2043.
4. Kumar T S P, Prabhu K N, *Met Trans* **20B** (1991) 717.
5. Prabhu K N, Griffiths W D, *Int J Cast Met. Res*, **14** (2001) 147.
6. Prabhu K N, Griffiths W D, *Materials Sci and Tech* **18** (2002) 804.
7. Loulou T, Artyukhin E A, Bardon J P, *Int J Heat and Mass Transfer* **42** (1999) 2119.
8. Loulou T, Artyukhin E A, Bardon J P, *Int. J Heat and Mass Transfer* **42** (1999) 2129.
9. Griffiths W D, *Met Mater Trans. B* **30** (1999) 473.
10. Ho K, Pehlke R D, *Met Trans B* **16** (1985) 585–596.
11. Beck J V, *J Heat Transfer*, **13** (1970) 703.
12. Huebner K H, Thornton E A, Byrom T G, *The Finite Element Methods for Engineers*, 3rd ed. John Wiley, New York (1995)
13. Poirier D R and Geiger G H, *Transport Phenomena in Materials Processing,* TMS, Pennsylvania, (1994).
14. Holman J P, *Heat Transfer*, 9th ed. Tata McGraw-Hill, New Delhi (2002)